Systematic Size Study of an Insect Antifreeze Protein and Its Interaction with Ice

Kai Liu,*† Zongchao Jia,‡ Guangju Chen,* Chenho Tung,† and Ruozhuang Liu*
*Department of Chemistry, Beijing Normal University, Beijing 100875, People's Republic of China; †Technical Institute of Physics and Chemistry, Chinese Academy of Sciences, Beijing 100101, People's Republic of China, and Graduate School of Chinese Academy of Sciences, Beijing 100039, People's Republic of China; and ‡Department of Biochemistry, Queen's University, Kingston, Ontario, K7L 3N6, Canada

ABSTRACT Because of their remarkable ability to depress the freezing point of aqueous solutions, antifreeze proteins (AFPs) play a critical role in helping many organisms survive subzero temperatures. The β-helical insect AFP structures solved to date, consisting of multiple repeating circular loops or coils, are perhaps the most regular protein structures discovered thus far. Taking an exceptional advantage of the unusually high structural regularity of insect AFPs, we have employed both semiempirical and quantum mechanics computational approaches to systematically investigate the relationship between the number of AFP coils and the AFP-ice interaction energy, an indicator of antifreeze activity. We generated a series of AFP models with varying numbers of 12-residue coils (sequence TCTxSxxCxxAx) and calculated their interaction energies with ice. Using several independent computational methods, we found that the AFP-ice interaction energy increased as the number of coils increased, until an upper bound was reached. The increase of interaction energy was significant for each of the first five coils, and there was a clear synergism that gradually diminished and even decreased with further increase of the number of coils. Our results are in excellent agreement with the recently reported experimental observations.

INTRODUCTION

Although antifreeze proteins (AFPs) have diverse primary sequences and three-dimensional structures, they all converge functionally to depress the freezing point of aqueous solutions. The mechanism by which AFP binds to ice and inhibits its growth is not fully understood, despite intensive research in the last 20 years. It is generally believed that AFPs produce antifreeze activity by adsorbing to a specific plane(s) on the surface of seed ice crystals and inhibiting their growth (Knight et al., 1991). AFP renders curved growth fronts of ice between the bound AFPs, which are less energetically favorable for growth, lowering the local freezing point. Because of our current inability to investigate AFP-ice interaction directly, numerous computational efforts have been made to better understand the interaction that is very specific to AFPs. In all these studies, relative AFP-ice interaction energy is an important parameter that can be computed. Although these are not of absolute values (in fact, maybe even very far from the actual value), they have been very useful as a relative indicator, which, for instance, is commonly used to compare different antifreeze activity of various AFPs, of the same AFP to various ice lattices, and locate ice-binding surface of AFP (e.g., see review of Madura et al., 2000; Chen and Jia, 1999; Cheng et al., 2002; Yang et al., 2003, among others).

The breadth of AFP structural diversity is considerable, ranging from highly repetitive α- and β-helical proteins to globular proteins wholly devoid of any obvious surface repetitiveness. In fact, the only common characteristic among the known AFPs appears to be their relatively small size (Jia and Davies, 2002). Why these proteins have evolved to the size they have is difficult to determine. Efforts to date to investigate AFP functionality have only made the question of AFP size more intriguing: hybrid constructs containing multiple AFP ice-binding domains have been shown to have higher activity than single-domain wild-type AFPs (Baardsnes et al., 2003; Nishimiya et al., 2003).

The AFP from the common yellow mealworm beetle (*Tenebrio molitor*, commonly known as TmAFP), a small antifreeze protein with molecular mass 8.4 KDa, is one of the most regularly structured proteins discovered (Liou et al., 2000, 1999; Graham et al., 1997) (Fig. 1). It is composed of seven disulfide-linked 12 amino acid loops whose backbone components and conserved side chains are almost identically oriented. On the conserved side of the TmAFP, threonine-cysteine-threonine (TCT) motifs are aligned to form a flat β-sheet (represented by the *green arrows* in Fig. 1) along one side of the molecule. These threonine residues project outwards in two precisely arranged parallel arrays. In terms of amino acid sequence, this AFP is very similar to the AFP from the pyrochroid beetle (*Dendroides canadensis,* DcAFP), which also consists of repetitive disulfide linked 12-residue coils (each coil in both of these AFPs has the conserved sequence TCTxSxxCxxAx) with Thr-Cys-Thr clustered at the ice-binding site. There are several known isoforms of these proteins with varying numbers of coils, ranging from a six-coil TmAFP isoform to a 10-coil DcAFP isoform (Duman et al., 1998; Graham et al., 1997; Liou et al.,

Submitted August 9, 2004, and accepted for publication November 3, 2004.
Address reprint requests to Prof. Guangju Chen, Dept. of Chemistry, Beijing Normal University, Beijing 100875, People's Republic of China. Tel.: 86-10-5880-7969; E-mail: gjchen@bnu.edu.cn.

0006-3495/05/02/953/06 $2.00
doi: 10.1529/biophysj.104.051169

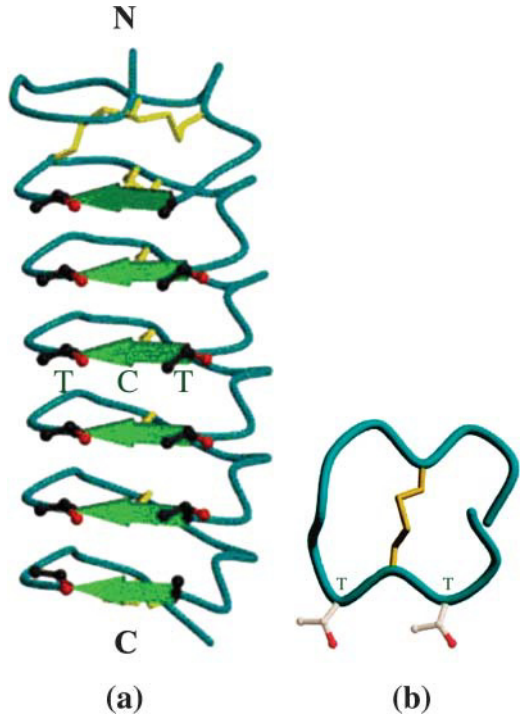

FIGURE 1 (*a*) Crystal structure of the seven-coil TmAFP. The green arrows indicate the β-sheet regions of this protein. TCT residues are represented by the ball-and-stick model. (*b*) A single coil with TCT residues shown. The two Thr residues are responsible for ice binding. In high-level QM calculations, only Thr groups are included in the computations due to prohibitive computing cost.

1999). As with most other proteins, activity is known to vary among AFP isoforms. An example of this is spruce budworm AFP (SbwAFP) (Graether et al., 2000), which is also a highly regular β-helical protein (though of opposite handedness to TmAFP) with a conserved TxT motif on its ice-binding face. For this AFP, the larger isoform 501 is ~3 times more active than the smaller isoform 337 (Leinala et al., 2002). Again, however, the relationship between protein size and antifreeze activity is simply not known, though these SbwAFP isoforms notwithstanding, it has been postulated that larger AFPs might not be as active due to a loss of structural regularity that is critical for ice binding (Jia and Davies, 2002).

In this article, we set out to investigate the optimal size of TmAFP as expressed by the number of repeating coils. Specifically, we have taken an exceptional advantage of the highly regular repeating coil structure of TmAFP, which provides a rare opportunity to systematically investigate the relationship between protein size and function. By systematically varying the number of coils, coupled with different computational approaches, we have obtained insights into the correlation between TmAFP size and its ice interaction. The nearly identical alignment of consecutive coils of these β-helical insect AFPs makes the investigation of the connection between AFP size and activity computationally feasible, as molecular models of varying sizes can be readily constructed by varying the numbers of these coils in a systematic and consistent way. Very recently, the number of coils in TmAFP has been altered experimentally, and antifreeze activity of the variants measured (Marshall et al., 2004). It is shown that ~9 coils provides optimal activity, which is, however, decreased upon further increase of the coils. This is in excellent agreement with this computational study where we observe the same trend.

METHODS

TmAFP-ice docking

The specific ice plane to which TmAFP has affinity {0100} was built using the HyperChem program (HyperChem, version 5.01). TmAFP was manually placed on this ice plane so that its Thr-Cys-Thr ice-binding surface was aligned toward the {0100} ice plane (Marshall et al., 2002; Leinala et al., 2002). The distances between the closest oxygen atoms of the ice plane and the binding surface atoms of the protein were 2 ~ 4 Å; these distances were favorable for interactions between the protein and ice. To better simulate actual AFP-ice interactions, the TmAFP-ice complex system was placed in a periodic box, in which there are in total 1030 atoms of TmAFP, 1440 atoms of ice, and 8538 atoms of water molecules. The solvent water molecules were treated as TIP3P models (Jorgensen et al., 1983).

Molecular mechanics method

Dynamic simulation and energy minimization using molecular mechanics (MM) were carried out to optimize the TmAFP-ice complex system. During the optimization and dynamics simulation processes, all atoms were allowed to move freely except the oxygen atoms in the ice. First, the TmAFP-ice complex was subjected to energy minimization using the conjugate gradient method with the AMBER force field (Weiner et al., 1984; Cornell et al., 1995). Second, molecular dynamics simulations were carried out for 350 ps at a constant temperature of 273 K without constraints. This step produced a quasi-static state for the TmAFP-ice complex system. Third, the system was further optimized by a final round of energy minimization; these structural optimizations were terminated with the convergence criterion of root mean-square gradient $\leq$0.000001 kcal/mol Å.

Semiempirical molecular orbital calculations

Based on the optimized TmAFP-ice complex, two semiempirical molecular orbital methods AM1 (Dewar et al., 1985) and PM3 (Stewart, 1989a,b) were used to study the relationship between TmAFP variants and the ice substrate. TmAFP variants include the intact TmAFP, one-coil deletion ''mutant'', two-coil deletion ''mutants'', etc. In other words, by systematically varying the number of the coils or the size of TmAFP, which is virtually not possible with a majority of the proteins, we would be able to estimate the ice interaction energy of TmAFP and its variants to eventually correlate the results with antifreeze activity.

Quantum mechanics calculations

To confirm the conclusions obtained by semiempirical molecular orbital methods, the higher level ab initio Hartree-Fock (HF) and density function B3LYP (Lee et al., 1988; Becke, 1993), which includes the electronic correlation energy, were further employed. Because the total number of atoms in the system was too large for comprehensive calculations, the interaction energy between the local effective functional groups (the

threonine residues of the protein and those parts of the ice that they contact) was computed by these quantum chemical methods with the basis set 6-31G. It has been established that the Thr-Cys-Thr motifs together constitute the ice-binding site (Jia and Davies, 2002), in which Cys points inward to form a disulfide bridge, whereas Thr residues project outward to achieve ice interaction. Thus the Thr residues, or local functional groups, represent the interaction between the protein and ice.

In the quantum calculations, HF/6-31G and B3LYP/6-31G were first employed, and then the solvent effects (SE) were considered by using the Onsager model (Wong et al., 1991, 1992). Finally, the basis set superposition errors (BSSE) (Jansen and Ros, 1969) and the solvent effects were simultaneously taken into account. All quantum calculations included in this work were performed with the Gaussian 98 software package (Frisch et al., 1998).

FIGURE 2 Examples of TmAFP models with different numbers of coils, aligned with the ice surface. For clarity, shown here are TmAFP models with one, three, five, and seven coils only.

RESULTS ANS DISCUSSION

Optimized geometry structure by molecular mechanics and molecular dynamics methods

Using molecular mechanics and molecular dynamics methods, we performed 350 ps of dynamics simulations on the AFP-ice complex and aqueous water molecules, and optimized the geometry of the resulting TmAFP-ice complex system. During the dynamics simulation process, the temperature of the system remained virtually unchanged during the entire simulation process. The average temperature was 273.05 K, with maximum and minimum temperatures of 277.92 K and 267.87 K, respectively. The total energy and the potential energy of the system decreased gradually in the first 200 ps of the simulation. The average total energy and average potential energy were −613391.12 kcal/mol and −622351.01 kcal/mol, respectively, with the standard deviation of −256.47 kcal/mol and −259.58 kcal/mol. Subsequently, the total energy and potential energy converged smoothly. The final average total energy and potential energy were −613750.53 kcal/mol and −622709.55 kcal/mol with the standard deviation of −46.15 kcal/mol and −65.18 kcal/mol, respectively. These results show that the TmAFP-ice complex system has reached a quasi-static state.

During the course of the molecular dynamics simulation of the TmAFP-ice interaction, the structure of the TmAFP, and especially the components on its β-surface, were well conserved. The RMSD between the Tm-AFP structure after molecular dynamics and the actual structure obtained by x-ray diffraction was only 1.879 Å.

Semiempirical molecular orbital calculations

We next studied the relationship between the size of the TmAFP molecule and the energy of interaction that occurs between it and its ice substrate by semiempirical molecular orbital calculation methods (AM1 and PM3). Antifreeze activity has been postulated to be partly determined by the strength of the AFP-ice interaction, or, in computational terms, by the AFP-ice interaction energy (Cheng et al., 2002). By systematically varying the number of repeating coils in TmAFP, we were able to calculate the interaction energies for a series of TmAFP molecules of increasing size. Based on the optimized TmAFP-ice system from MM, we began with a model possessing only the first coil (i.e., coils 2–7 were deleted), as shown in Fig. 2. The interaction energy between the first coil and the ice lattice was calculated using the semiempirical molecular orbital methods mentioned above. Additional coils were then added one by one until all seven coils were included and the calculation was repeated after every coil addition.

Using the semiempirical molecular orbital methods, we calculated the interaction energy as follows: $\Delta E_{\text{interaction}} = E_{\text{complex}} - (E_{\text{AFP}} + E_{\text{ICE}})$ (Chen and Jia, 1999). As is evident in Fig. 3, the interaction energy increased gradually as more coils were included, but then slowed down and eventually reached a plateau upon further increase of the coils. The interaction energy does not increase indefinitely, nor is it proportional to the number of the coils when it is further increased. Only for the first ~5 coils, the increase in interaction energy corresponds well with the number of coils. Hence, the increase of interaction energy is significant for the

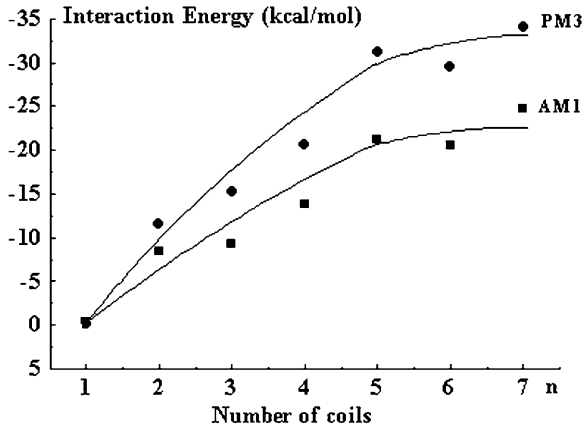

FIGURE 3 Total interaction energy versus the number of coils as calculated by AM1 and PM3 semiempirical methods.

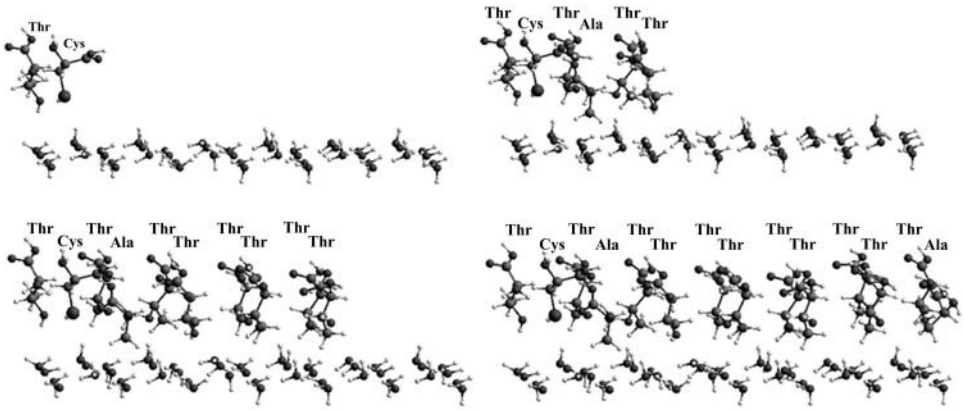

FIGURE 4 Detailed view of specific TmAFP residues that interact with the ice surface. Similar to Fig. 2, for clarity shown here are residues from TmAFP models containing one, three, five, and seven coils only.

shorter versions of the insect AFP. However, this trend did not last after ~5 coils. The energy increase slowed down considerably. We thus suggest that there is an optimal limit to the number of Thr-Cys-Thr coils or the size of the protein. Excessive number of coils would not only ''cost'' more to synthesize, but also would not offer proportionally increased ice interaction and consequently antifreeze activity.

Quantum mechanics calculations

To better understand the upper bound on the interaction energy, we performed higher-level quantum mechanics (QM) calculations including ab initio HF and density functional theory (B3LYP) methods with the basis set 6-31G. Because the number of atoms contained in the TmAFP-ice complex systems is too large for these QM calculations, we focused only on the functional groups in each coil of the TmAFP (i.e., the threonine residues responsible for ice binding), while keeping the rest of the protein in its optimized conformation (Fig. 4). The interaction energies for the various TmAFP-ice complex calculated using QM under different conditions (gas phase only, solvent effect considered, solvent effect and BSSE considered simultaneously) are shown in Fig. 5. The trend of interaction energy is the same using different methods and under different conditions, though there is some difference in the exact values of the interaction energies. When the solvent and BSSE are included simultaneously, the values are the smallest and appear to be most reasonable. Our primary objective here is to compare the ice interaction energies of TmAFP variants containing varying number of coils instead of the absolute energy values. Comparing Figs. 3 and 5, the same plateauing effect obtained using the semiempirical methods also occurs using both the ab initio and density functional theory methods. The fact that the results from both the semiempirical and the quantum mechanics methods follow the same leveling-off trend helps lend credibility to both methodologies, and, in particular, adds a measure of validity to the quantum mechanics calculations, where the model had to be simplified to focus solely on interactions between AFP functional groups and ice. Furthermore, because the results from both methodologies tracked together, and because the QM calculations focused solely on functional group interactions, it is reasonable to conclude that the interaction between protein and ice is essentially localized to these functional groups.

We further examined the interaction energy of individual coils, represented by $(E_n - E_{n-1})$, where E_n and E_{n-1} correspond to the interaction energy of the systems containing N and $N - 1$ number of coils. The difference between them represents the interaction energy of an individual coil. Table 1 clearly shows that there is a profound synergistic response to adding coils in the early stages. However, this trend only lasts until the fifth coil, after which the synergy is no longer observed. This intriguing observation demonstrates that there is a limit to the synergistic effect of coil additions.

Theoretical models containing additional coils

Because of the extreme regularity of the TmAFP structure, it is possible to construct larger TmAFP models containing additional coils, and to subject these models to the same set of molecular mechanism and quantum mechanism calculations

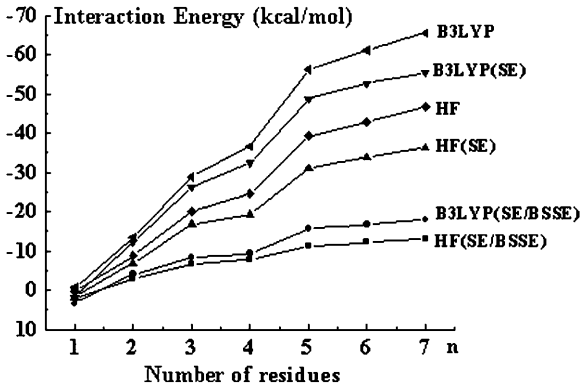

FIGURE 5 Total interaction energy calculated with QM methods. SE donates the calculations that included solvent effects.

TABLE 1 Interaction energies of individual residues (SE donates the calculations involving solvent effects)

	$E_n - E_{(n-1)}$ (kcal/mol)			
N- (N − 1)	HF/6-31G	HF/6-31G (SE)	B3LYP/6-31G	B3LYP/6-31G (SE)
2-1	−9.023	−8.556	−12.706	−10.321
3-2	−11.209	−9.952	−15.414	−14.010
4-3	−4.544	−2.507	−7.874	−6.211
5-4	−14.732	−11.871	−19.468	−16.346
6-5	−3.723	−2.739	−4.989	−3.890
7-6	−3.802	−2.459	−4.330	−2.758

that were performed on all of the other models. We took coils 5, 6, and 7 from the optimized original seven-coil model and carefully fused them to the latter structure. It is noted that the three coils (5, 6, and 7) had been already optimized as part of the original structure. The connection between the seven-coil model and the three-coil additional structure was carefully made according to virtually the same connection geometry of other coils because of the highly regular TmAFP structure. Bond angles, bond length, and dihedral angles were all taken into account in this exercise. The resulting model was subjected to further energy minimization and is shown in Fig. 6.

As was done with the TmAFP models containing 1–7 coils, the semiempirical and quantum mechanics calculations were systematically performed for the variants by sequentially deleting coil(s) from the 10-coil model. As is evident in Fig. 7, interaction energy increases steadily and reaches its maximum with the models that contain ~8 coils before starting to decrease. Obviously, with more coils included, the gain in interaction energy not only becomes no longer proportional to the number of coils but also there is even a decrease. This observation is very close to the recently reported experimental results in which the nine-coil variant had the highest activity, whereas further increase of coils actually impaired the antifreeze activity (Marshall et al., 2004). Thus there is a close agreement between the theoretical and experimental results, although the theoretical efforts were carried out without any prior knowledge of the experimental work.

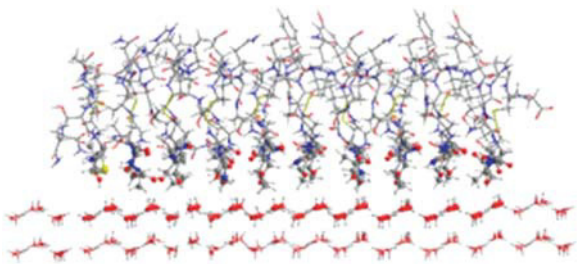

FIGURE 6 Model structure of the 10-coil isoform of TmAFP interacting with the ice lattice. TCT residues are shown in ball-and-stick mode.

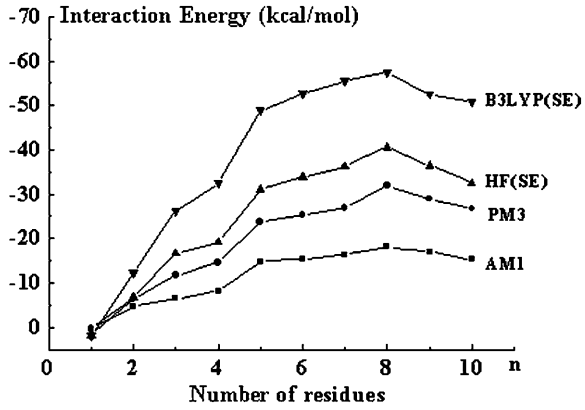

FIGURE 7 Total interaction energy of TmAFP models containing up to 10 coils. SE denotes the calculations that include solvent effects.

CONCLUSION

In this article, we employed both semiempirical and quantum mechanics computational approaches to systematically investigate the correlation between the numbers of coils in TmAFP constructs and the AFP-ice interaction energy. The extreme structure regularity of TmAFP rendered systematic size variation (number of coils) possible. By systematically examining constructs containing between 1 and 10 coils, we found that the AFP-ice interaction energy increases with the increased number of coils up to a certain point, after which there is actually a decrease. This observation is in agreement with experimental results.

This work was funded by Science Foundation of National Science Foundation of China (grant Nos. 20271009, 20231010, and 30228006), the Major State Basic Research Development Programs (grant Nos. G2000078100 and G2004CB719900), and the Key Projection by the Ministry of Education. Z.J. is supported by Canadian Institutes of Health Research and is also a Canada Research Chair in Structural Biology.

REFERENCES

Becke, A. D. 1993. Density-functional thermochemistry. III. The role of exact exchange. *J. Chem. Phys.* 98:5648–5652.

Baardsnes, J., M. J. Kuiper, and P. L. Davies. 2003. Antifreeze protein dimer: when two ice-binding faces are better than one. *J. Biol. Chem.* 278:38942–38947.

Chen, G. J., and Z. Jia. 1999. Ice-binding surface of fish type III antifreeze. *Biophys. J.* 77:1602–1608.

Cheng, Y. H., Z. Y. Yang, H. W. Tan, R. Z. Liu, G. J. Chen, and Z. Jia. 2002. Analysis of ice-binding sites in fish type II antifreeze protein by quantum mechanics. *Biophys. J.* 83:2202–2210.

Cornell, W. D., P. Cleplak, C. I. Bayly, I. R. Gould, K. M. Merz, D. M. Ferguson, D. C. Spellmeyer, T. Fox, J. W. Caldwell, and P. A. Kollman. 1995. A second generation force field for the simulation of proteins, nucleic acids, and organic molecules. *J. Am. Chem. Soc.* 117:5179–5197.

Dewar, M. J. S., E. G. Zoebisch, E. F. Healy, and J. J. P. Stewart. 1985. AM1: a new general purposes quantum mechanical model. *J. Am. Chem. Soc.* 107:3902–3909.

Duman, J. G., N. Li, D. Verleye, F. W. Goetz, D. W. Wu, C. A. Andorfer, T. Benjamin, and D. C. Parmelee. 1998. Molecular characterization and sequencing of antifreeze proteins from larvae of the beetle *Dendroides canadensis*. *J. Comp. Physiol. [B]*. 168:225–232.

Frisch, M. J., G. W. Trucks, H. B. Schlegel, G. E. Scuseria, M. A. Robb, J. R. Cheeseman, V. G. Zakrzewski, J. A. Montgomery, Jr., R. E. Stratmann, J. C. Burant, S. Dapprich, J. M. Millam, A. D. Daniels, K. N. Kudin, M. C. Strain, O. Farkas, J. Tomasi, V. Barone, M. Cossi, R. Cammi, B. Mennucci, C. Pomelli, C. Adamo, S. Clifford, J. Ochterski, G. A. Petersson, P. Y. Ayala, Q. Cui, K. Morokuma, D. K. Malick, A. D. Rabuck, K. Raghavachari, J. B. Foresman, J. Cioslowski, J. V. Ortiz, B. B. Stefanov, G. Liu, A. Liashenko, P. Piskorz, I. Komaromi, R. Gomperts, R. L. Martin, D. J. Fox, T. Keith, M. A. Al-Laham, C. Y. Peng, A. Nanayakkara, C. Gonzalez, M. Challacombe, P. M. W. Gill, B. G. Johnson, W. Chen, M. W. Wong, J. L. Andres, M. Head-Gordon, E. S. Replogle, and J. A. Pople. 1998. GAUSSIAN 98 (Revision A.9). Gaussian Inc., Pittsburgh, PA.

Graether, S. P., M. J. Kuiper, S. M. Gagne, V. K. Walker, Z. Jia, B. D. Sykes, and P. L. Davies. 2000. β-helix structure and ice-binding properties of a hyperactive antifreeze protein from an insect. *Nature*. 406:325–328.

Graham, L. A., Y. C. Liou, V. K. Walker, and P. L. Davies. 1997. Hyperactive antifreeze protein from beetles. *Nature*. 388:727–728.

Jansen, H. B., and P. Ros. 1969. Non-empirical molecular orbital calculations on the protonation of carbon monoxide. *Chem. Phys. Lett*. 3:140–143.

Jia, Z., and P. L. Davies. 2002. Antifreeze proteins: an unusual receptor-ligand interaction. *Trends Biochem. Sci*. 27:101–106.

Jorgensen, W. L., J. Chandrasekhar, and J. D. Madura. 1983. Comparison of simple potential functions of simulating liquid water. *J. Chem. Phys*. 79:926–935.

Knight, C. A., C. C. Cheng, and A. L. DeVries. 1991. Adsorption of α-helical antifreeze peptides on specific ice crystal surface planes. *Biophys. J*. 59:409–418.

Lee, C., W. Yang, and R. G. Parr. 1988. Development of the Colle-Salvetti correlation-energy formula into a functional of the electron density. *Phys. Rev. B*. 37:785–789.

Leinala, E. K., P. L. Davies, D. Doucet, M. G. Tyshenko, V. Walker, and Z. Jia. 2002. A β-helical antifreeze protein isoform with increased activity. Structural and functional insights. *J. Biol. Chem*. 277:33349–33352.

Liou, Y. C., A. Tocilj, P. L. Davies, and Z. Jia. 2000. Mimicry of ice structure by surface hydroxyls and water of a β-helix antifreeze protein. *Nature*. 406:322–324.

Liou, Y. C., P. Thibault, V. K. Walker, P. L. Davies, and L. A. Graham. 1999. A complex family of highly heterogeneous and internally hyperactive antifreeze proteins from the beetle *Tenebrio molitor*. *Biochemistry*. 38:11415–11424.

Marshall, C. B., M. E. Daley, L. A. Graham, B. D. Sykes, and P. L. Davies. 2002. Identification of the ice-binding face of antifreeze protein from *Tenebrio molitor*. *FEBS Lett*. 529:261–267.

Marshall, C. B., M. E. Daley, B. D. Sykes, and P. L. Davies. 2004. Enhancing the activity of a β-helical antifreeze protein by the engineered addition of coils. *Biochemistry*. 43:11637–11646.

Madura, J. D., K. Baran, and A. Wierzbicki. 2000. Molecular recognition and binding of thermal hysteresis proteins to ice. *J. Mol. Recognit*. 13:101–113.

Nishimiya, Y., S. Ohgiya, and S. J. Tsuda. 2003. Artificial multimers of the type III antifreeze protein. Effects on thermal hysteresis and ice crystal morphology. *J. Biol. Chem*. 278:32307–32312.

Stewart, J. J. P. 1989a. Optimization of parameters for semi-empirical methods. I. Method. *J. Comput. Chem*. 10:209–220.

Stewart, J. J. P. 1989b. Optimization of parameters for semi-empirical methods. II. Application. *J. Comput. Chem*. 10:221–264.

Weiner, S. J., P. A. Kollman, D. A. Case, U. C. Singh, C. Ghio, G. Alagono, J. S. Profeta, and P. Weiner. 1984. A new force field for molecular mechanical simulation. *J. Am. Chem. Soc*. 106:765–784.

Wong, M. W., M. J. Frisch, and K. B. Wiberg. 1991. Solvent effects. 1. The mediation of electrostatic effects by solvents. *J. Am. Chem. Soc*. 113:4776–4782.

Wong, M. W., K. B. Wiberg, and M. J. Frisch. 1992. Solvent effects. 2. Medium effect on the structure, energy, charge density, and vibrational frequencies of sulfamic acid. *J. Am. Chem. Soc*. 114:523–529.

Yang, Z., Y. Zhou, K. Liu, Y. Cheng, R. Liu, G. Chen, and Z. Jia. 2003. Computational study on the function of water within a β-helix antifreeze protein dimer and in the process of ice-protein binding. *Biophys. J*. 85:2599–2605.